

# Pan-human consensus genome significantly improves the accuracy of RNA-seq analyses.

Benjamin Kaminow<sup>1,2</sup>, Sara Ballouz<sup>1,3,4</sup>, Jesse Gillis<sup>1</sup>, Alexander Dobin<sup>1</sup>

Jesse Gillis: [jgillis@cshl.edu](mailto:jgillis@cshl.edu); Alexander Dobin: [dobin@cshl.edu](mailto:dobin@cshl.edu)

<sup>1</sup>Cold Spring Harbor Laboratory, Cold Spring Harbor, NY, USA; <sup>2</sup>Tri-Institutional Ph.D. Program in Computational Biology and Medicine, Weill Cornell Graduate School of Medical Sciences, New York, NY, USA; <sup>3</sup>Garvan-Weizmann Centre for Cellular Genomics, Garvan Institute of Medical Research, Darlinghurst, NSW; <sup>4</sup>School of Medical Sciences, University of New South Wales, Sydney, NSW

**Running Title:** Consensus genome improves the accuracy of RNA analyses

**Keywords:** consensus genome, genome variation, RNA-seq

The Human Reference Genome serves as the foundation for modern genomic analyses. However, in its present form, it does not adequately represent the vast genetic diversity of the human population. In this study, we explored the consensus genome as a potential successor of the current reference genome and assessed its effect on the accuracy of RNA-seq read alignment. In order to find the best haploid genome representation, we constructed consensus genomes at the pan-human, super-population, and population levels, utilizing variant information from the 1000 Genomes project. Using personal haploid genomes as the ground truth, we compared mapping errors for real RNA-seq reads aligned to the consensus genomes versus the reference genome. For reads overlapping homozygous variants, we found that the mapping error decreased by a factor of ~2-3 when the reference was replaced with the pan-human consensus genome. We also found that using more population-specific consensus genomes resulted in little to no increase overusing the pan-human consensus, suggesting a limit in the utility of incorporating more specific genomic variation. Replacing reference with consensus genomes impacts functional analyses, such as differential expressions of isoforms, genes, and splice junctions.

## Introduction

In 2003, 15 years of work culminated with the International Human Genome Sequencing Consortium publishing the first finished version of the Human Reference Genome (<https://www.genome.gov/human-genome-project/Completion-FAQ>; International Human Genome Sequencing Consortium 2004). Despite the utility and continuous improvements over the years, it is still not without flaws – primarily the lack of variation information. Around 93% of the current GRCh38 assembly is composed of DNA from just 11 individuals (<https://www.ncbi.nlm.nih.gov/grc/help/faq/>; International Human Genome Sequencing Consortium 2001). Because such a large portion of the reference comes from such a small pool of individuals, it does not adequately represent the vast diversity present in the human population (Chen and Butte 2011; Rosenfeld et al. 2012; Sherman et al. 2019). To explore and capture human diversity, researchers have continued sequencing thousands of genomes. The first of such projects, the 1000 Genomes Project, sequenced 2,504 individuals across 26 populations. Overall, it was estimated that ~3,000 genomes would be necessary to capture the most common variants (Ionita-Laza et al. 2009), while structural variation present in the human populations has challenged this (Berlin et al. 2015). One particularly glaring example was shown in a recent construction of an African pan-genome, which contained almost 300M bases of DNA not seen in GRCh38 (Sherman et al. 2019). This lack of variation information negatively affects all kinds of genomic analyses that utilize the reference, such as disease studies and GWAS analyses (Buchkovich et al. 2015; Castel et al. 2015; Chen and Butte 2011; Rosenfeld et al. 2012; Sherman et al. 2019; Stevenson et al. 2013). However, despite the ubiquity of RNA-seq alignment and quantification, the improvements in mapping from using a more diverse reference have not been shown.

While graph genomes are theoretically capable of encapsulating all observed variation information (Church et al. 2015; Garrison et al. 2018; Paten et al. 2017; Rakocevic et al. 2019; Sirén et al. 2021; Valenzuela et al. 2018), it remains challenging to use these tools for large scale expression analysis such as in RNA-seq quantification. In prior work, we proposed using a consensus genome to inherently capture common variation while still retaining the structure and functionality of the current reference assembly (Ballouz et al. 2019). A consensus genome is a linear haploid genome that

incorporates population variation information by replacing all minor alleles in the reference genome with the major allele of that variant (Balasubramanian et al. 2011; Ballouz et al. 2019; Barbitoff et al. 2018; Dewey et al. 2011; Karthikeyan et al. 2016; Pritt et al. 2018; Shukla et al. 2019) (Figure 1A). Because allele frequencies must be defined with respect to a population, a consensus genome is representative of the population used to define the major and minor alleles. Prior work has shown that using a consensus genome can have positive effects on variant calling (Karthikeyan et al. 2016; Pritt et al. 2018; Shukla et al. 2019), and the construction of population-specific consensus genomes has been a major goal of multiple projects (Cho et al. 2016; Fakhro et al. 2016; Higasa et al. 2016; Sherman et al. 2019; Takayama et al. 2021). Additionally, replacing the current reference genome with a consensus genome in existing analysis pipelines is straightforward since the consensus genome is still a linear haploid sequence.

Here, we seek to answer the question of which linear reference representation is best for RNA-seq mapping and downstream analyses. We considered several consensus genomes, built by replacing all minor alleles in the reference with the major alleles at different population levels: pan-human, super-population, and population. To work with consensus genomes, we developed ConsDB to construct pan-human and population-level consensus, and STAR-consensus to streamline RNA-seq mapping to consensus genomes. We defined the ground truth by mapping the individuals' RNA-seq reads to their personal haploid genomes and evaluated the mapping accuracy improvements arising from replacing the GRCh38 reference with the pan-human consensus, super-population, or population consensus genomes. We found that for all individuals, the pan-human consensus decreased the mapping error from the reference by ~2-3 fold, while the super-population and population consensus did not perform significantly better than the pan-human consensus. To assess the functional impact, we measured errors in splice junction expression quantification for different genome representations with respect to the ground truth of the personal genome. We again found that the pan-human consensus offers an improvement over the reference, with ~5 times as many splice junctions having a larger quantification error for the reference than for the pan-human consensus.

## Results

Pan-human consensus captures the majority of population deviation from the reference.

The construction of consensus genomes requires population allele frequency information. Currently, several databases contain this information (The 1000 Genomes Project Consortium 2015; Church et al. 2015; Karczewski et al. 2020; Sherry et al. 2001). In this study, we utilized the 1000 Genomes Project database, which was established to discover and catalog human genome variant information (The 1000 Genomes Project Consortium 2015; Clarke et al. 2017). To avoid population bias, the individuals genotyped in the 1000 Genomes Project were selected to create an even population distribution across 26 populations, which are grouped into 5 super-populations (The 1000 Genomes Project Consortium 2015) (Figure 1B). This balance between the different populations means that the 1000 Genomes Project database is well-suited for creating a draft pan-human consensus genome, while other popular databases are more skewed towards specific populations and will therefore produce a biased pan-human consensus genome. Additionally, the information from the 1000 Genomes Project is publicly available through the International Genome Sample Resource (IGSR) and can be downloaded in the form of VCF files, which contain variant genotype information for all individuals (The 1000 Genomes Project Consortium 2015).

We constructed three types of consensus genomes based on the various population levels present in the 1000 Genomes Project: a pan-human consensus genome, a super-population consensus genome, and a population consensus genome (Figure 1B). For the pan-human consensus, we calculated allele frequency using genotype information from all individuals present in the database. For the super-population and population consensus, we used genotype information from all individuals of a given super-population or population. For the 8 individuals whose RNA-seq data we utilized in this study, we used the consensus genomes built from the super-population and population each individual belongs to.

To construct these consensus, we replaced all minor alleles (alleles with a population allele frequency  $AF < 0.5$ ) present in the reference with the major alleles ( $AF > 0.5$ ). This procedure is applied to both single nucleotide variants and insertions/deletions. For simplicity, we omit overlapping indels. We will call these variants replaced in the reference the major allele replacements (MAR).

The release of the 1000 Genomes database that we used contained only biallelic variants, i.e., each variant had exactly one minor allele and one major allele. Additionally, it only contained SNPs and small insertions and deletions ( $< 50$  bp), while large structural variants were not considered in this study. Although SVs are a large source of genomic variation, they are understudied and not sufficiently cataloged to be used in consensus genomes due to mapping and classification difficulties (Mahmoud et al. 2019).

In order to facilitate working with the large VCF files of the 1000 Genomes Project database, we developed ConsDB, a Python package that provides a convenient, class-based interface to work with the large number of variants contained in the 1000 Genomes Project database. It also provides the main script with several run modes to perform common tasks associated with consensus genomes, such as constructing the consensus genome VCF files used in this study. ConsDB operates using a simple workflow (Figure 1C). The first step is downloading the database VCF files. For this study, we used the 1000 Genomes Project, but ConsDB is also capable of parsing gnomAD VCF files. The next step is for ConsDB to parse the database VCF files and save them in the ConsDB format. At this point, files from different databases (if multiple databases are being used) can be combined into one file per chromosome. Finally, ConsDB uses these parsed files to generate the end result, in this case, a VCF file defining a consensus genome.

One of ConsDB's main benefits is that it facilitates working with large variant databases. While tools such as BCFtools (Danecek et al. 2021) can also construct consensus genomes from VCF files, creating a population-specific consensus requires building complex expressions for variant inclusion that may prove difficult for some users. ConsDB is designed to be easy to use and allows the construction of population-specific consensus using just a single additional file with

population information. ConsDB also exposes a powerful and easy-to-use backend that allows more advanced users to incorporate its capabilities into their own pipelines.

The personal haploid genomes were constructed using the individual genotypes from the 1000 Genomes Project database. For each individual, all homozygous variants that differ from the reference were inserted into the reference. Additionally, all heterozygous alleles were randomly chosen with a probability of 0.5 to be included or excluded. Although these haploid personal genomes are a crude approximation of the actual diploid genome, they are sufficient for comparison of mapping accuracy between haploid consensus and the haploid reference, and thus we used them to define the ground truth for RNA-seq mapping in this study.

Figure 1D shows the number of minor alleles in the GRCh38 reference that must be replaced with the major alleles for each of the super-population consensus genomes. The European consensus is the most similar to the reference, and it still requires ~2.1 million SNP and indel corrections from the reference. Other super-population consensus contain even larger numbers of major allele deviations from the reference, with the East Asian consensus differing most from the reference. We note that such a large number of minor alleles in the reference with respect to any population stems from its construction, which utilized sequences from only one individual for most of the genomic loci, and thus incorporated individual-specific low-frequency alleles.

In Figure 1E, we compute intersections of the MARs in the pan-human, African super-population, and Yoruban population consensus genomes. The pan-human consensus shares most of the major alleles with the super- and population consensus (~1.5M), while the latter two share ~400k MARs not present in the pan-human consensus. The pan-human consensus contains ~300k MARs not present in either super- or population consensus. Finally, the Yoruban population consensus has ~50k unique MARs. The intersections of MARs look similar for other populations (Supplementary Figures S1-2) and personal homozygous variants (Supplementary Figures S3-5). Figure 1F shows the intersections between the MARs for the pan-human consensus and three super-population consensus. The MARs shared by all four of these genomes make up the largest group, containing ~1.2M MARs and representing well over half

of the MARs in any one genome. This group is more than 3 times as large as the next largest group, demonstrating that most of the population deviation from the reference is captured in the pan-human consensus.

### Consensus genomes significantly improve RNA-seq mapping.

Next, we analyzed to what extent the consensus genomes improve RNA-seq mapping accuracy. The RNA-seq reads were obtained from the Human Genome Structural Variation Consortium, which sequenced three father-mother-daughter trios from the 1000 Genomes Project (Fairley et al. 2020). One of these individuals (HG00514 from the East Asian trio) is not present in the database version used in this analysis and was excluded from our analyses.

To simplify alignment to the consensus genome, we developed STAR-consensus, an extension to the RNA-seq aligner STAR (Figure 2A) (Dobin et al. 2013). It imports variants from a VCF file and incorporates them into the reference genome sequence, thus creating a transformed genome for mapping. Importantly, after mapping the reads to the transformed genome, STAR-consensus can reverse the alignment coordinates back to the original reference genome coordinates. This transformation is non-trivial when insertion or deletion variants are included and allows performing all downstream analyses in the reference coordinate system. Such an approach is an incremental step towards taking advantage of the consensus genome while at the same time utilizing the conventional coordinate system.

The summary statistics for alignments to the reference and consensus genomes are presented in Supplementary Table S1. The changes in the overall mapping rates are marginal because only a small proportion of reads overlap the MARs. The effect is more pronounced for reads that overlap personal homozygous SNPs (2.2% of all reads): the unique mapping rate for such reads increases from 92.6% to 94.5%, while the mismatch error rate is reduced from 1.3% to 0.5%. Similar effects are observed for reads overlapping homozygous indels, which constitute only 0.15% of all reads.

To assess the error rate, we needed to compare the read mappings in the various genomes to ground truth. However, because the true mapping location of these reads is unknown, we used the personal haploid genome alignments as the ground truth. The personal haploid genomes correctly incorporate individual homozygous variants and thus can serve as a first-order approximation to the actual diploid personal genomes. Since typically both heterozygous alleles are present

in RNA-seq reads, choosing one of them randomly (Supplementary Figure S36) should be neutral for alignment accuracy on average (i.e., it should not make the alignment better or worse). Hence, the haploid genome is a good proxy for the actual personal diploid genome as it improves the alignment accuracy of homozygous variants while not affecting the heterozygous variants.

We classified mapping errors into five types based on the change of the read's alignment status in the reference/consensus genome compared to the ground truth (Figure 2B). The different error types are: reads that are mapped uniquely in the personal genome but mapped to multiple loci in the other genome (Unique to Multiple), reads that are mapped to multiple loci in the personal genome but mapped uniquely in the other genome (Multiple to Unique), reads that mapped to the personal genome but not to the other genome (Mapped to Unmapped), reads that didn't map to the personal genome but did map to the other genome (Unmapped to Mapped), and reads that mapped uniquely in both genomes but to different positions (Different Mapping Loci). The mapping error rate for an error type is defined as the number of erroneously mapped reads normalized by the total number of reads from an individual.

For each individual, we calculated the error rates for mapping to the reference and their respective consensus genomes (pan-human, super-population, population). Figure 2C shows the overall error rates for each error type for the individual NA19238. The most significant error comes from the reads that switch from mapping uniquely in the personal genome to mapping to multiple loci in the reference/consensus genomes, followed by reads that map to multiple loci in the personal genome but map uniquely in the reference/consensus.

We also separately plotted the error rate for reads that overlap indel variants (Supplementary Figure S6), which are very small compared to the overall error rates in Figure 2C. These plots look similar for the other individuals (Supplementary Figures S7-20).

Figure 2D shows the overall mapping error rate for all eight individuals, summed over the five error types. We see a noticeable decrease in the error rate when the reference genome is replaced with the pan-human consensus. Additionally, increasing population specificity to the super-population or population consensus does not result in a



significant further reduction of the error rate. This trend mirrors the observation about the minor alleles discussed above (Figures 1E-F) and supports the conjecture that the majority of the mapping accuracy improvement is captured by the pan-human consensus, with little additional benefit from the super-population or population consensuses.

Replacement of the minor alleles in the reference with the major alleles in the consensus can only correct the mapping errors caused by the homozygous alternative alleles in an individual. Of course, the actual individual genome is diploid and contains millions of heterozygous variants (i.e., both the major and minor alleles are present), which cannot be truthfully represented in a haploid reference or consensus genome. To elucidate this issue, we defined the homozygous mapping error rate as the number of erroneously mapped reads that overlap homozygous variants normalized by the total number of reads overlapping homozygous variants for an individual. The homozygous mapping error rate shows the effect of different genomes, specifically on read alignments that can be affected by these genomes. Because the genomes used in this study are all haploid, we do not expect reads that overlap heterozygous variants to be significantly affected by the specific genome used.

We plotted the homozygous mapping error rates for the individual NA19238 (for each error type) in Figure 2E and all eight individuals (summed over all error types) in Figure 2F. Compared to Figures 2C-D, the homozygous error rates (Figures 2E-F) show a much steeper decrease when the reference genome is replaced with the pan-human consensus. Additionally, the heterozygous error rate is higher than the homozygous error rate and stays relatively constant across all genomes (Supplementary Figures S21-28). This supports the notion that consensus genomes significantly improve the mapping accuracy of the reads that overlap homozygous variants; however, owing to their haploid nature, they cannot improve the alignment of the reads overlapping heterozygous loci.

We have investigated the robustness of our results with respect to the consensus allele definition (Supplementary Figure S30). We see significant improvement in mapping accuracy even for relaxed (AF > 40%) or stringent (AF > 60%) major allele frequency thresholds, only slightly different from the standard definition (AF > 50%). These results demonstrate that the consensus genome benefits do not strongly depend on the precise definition of the consensus alleles or the

databases used to calculate allele frequencies. This is not surprising since the main accuracy improvements are due to the elimination of relatively rare minor alleles from the reference. We find the same trends for RNA-seq data for 100 European and African individuals sequenced by the Geuvadis (Fairley et al. 2020; Lappalainen et al. 2013) consortium (Supplementary Figure S29).

In the calculations above, the error rates were defined relative to the personal genome alignments, which were considered the ground truth. To corroborate our findings, we simulated reads from the personal genomes of each individual and calculated the error rate with respect to the true read loci (Figures 2G-H). The simulated error rates exhibit a significant reduction when switching from the reference to the pan-human consensus and a much smaller decrease for super-population and population consensus, very similar to the results obtained for real RNA-seq data (Figures 2E-F).

To further test the robustness and generalizability of these results, we also analyzed the mapping error rates reduction in consensus genomes for another popular RNA-seq aligner, HISAT2 (Kim et al. 2019). Supplementary Figure S31 shows that the trends for HISAT2-mapped reads are qualitatively similar to our STAR results (Figure 2). These results demonstrate that consensus genomes will be advantageous regardless of the alignment algorithm used.

### Mapping RNA-seq reads to unrelated consensus genomes outperforms the reference.

We investigated the effects of mapping an individual's RNA-seq reads to consensus genomes of different populations (Figure 3A) and other personal haploid genomes (Figure 3C). We used the same reads, individuals, and genomes as previously discussed and mapped all individuals to all genomes. The homozygous mapping error rate is calculated as before and is shown in Figures 3B-D.

As expected, Figure 3B shows that the unrelated consensus genomes perform worse than both the related population consensus and the pan-human consensus because each population consensus contains many major alleles unique to that population. On the other hand, unrelated consensus genomes still perform better than the reference. This is explained by the fact that the reference contains a large number of minor alleles specific to the individuals who contributed to the reference assembly. Conversely, the personal genomes of unrelated individuals are unlikely to share

many MARs. This is illustrated in Figure 3D: the mapping error rate to personal genomes from different populations is higher than mapping to the pan-human consensus and is comparable with mapping to the reference. Even mapping to the unrelated individual genome from the same population (Mother to Father and Father to Mother) does not improve the accuracy significantly. However, since the daughter in each trio will share many of her MARs with her parents, we see the error rates for mapping daughters' RNA-seq reads to their parents' genome (and vice versa) slightly better than mapping to the pan-human consensus.

The results demonstrate that the reference genome performs worse than any consensus genome, even consensus from a different population. The accuracy of mapping to the reference is comparable to mapping to unrelated personal genomes. On the other hand, the pan-human consensus outperforms mapping to the unrelated individual genomes of the same or different population, and its performance is comparable with mapping to the genomes of related individuals (parent to child).

### Major allele replacements affect gene sequences.

The distribution of MARs in the exons of annotated genes is shown in Figure 4A. Overall, 12k protein-coding and 11k non-coding genes contain at least one exonic MAR. Approximately 50% of the protein-coding genes containing MARs have known disease associations (Piñero et al. 2016). While most genes contain fewer than 10 MARs, 235 genes carry more than 10 MARs. These results demonstrate that the many transcript sequences in the current reference contain minor alleles, which are replaced with more representative major alleles in the consensus genome. Of course, even larger numbers of MARs per gene are located in the intronic regions (Supplementary Figure S32).

To investigate the genomic mechanisms underlying these mapping errors, we classified the genomic loci of the error-causing variants by overlapping error-causing reads with the GENCODE v29 annotations. Only a small proportion of the error-causing variants occur in the coding regions, while most are located in the intronic regions, followed by UTR and intergenic regions (Figure 4B). Because poly(A)<sup>+</sup> RNA-seq reads should generally not map to introns, these errors are likely attributable to reads switching between being uniquely mapped and mapping to multiple locations (Unique to

Multiple and Multiple to Unique error types). This corresponds with the previous observation that the largest sources of errors were the Unique to Multiple and Multiple to Unique error types.

The distribution of MARs in the exons of annotated genes is shown in Figure 4A. Overall, 12k protein-coding and 11k non-coding genes contain at least one exonic MAR. Approximately 50% of the protein-coding genes containing MARs have known disease associations (Piñero et al. 2016). While most genes contain fewer than 10 MARs, 235 genes carry more than 10 MARs. These results demonstrate that the many transcript sequences in the current reference contain minor alleles, which are replaced with more representative major alleles in the consensus genome. Of course, even larger numbers of MARs per gene are located in the intronic regions (Supplementary Figure S32).

### Major allele replacements affect gene expression.

Here, we exemplify the effects of replacing the reference with a consensus genome on gene expression in a single-cell RNA-seq dataset. The prevalent droplet-based single-cell sequencing technologies allow studying the differential transcriptomic programs between cell types. Since a large proportion of reads generated by these technologies originate from UTRs and introns, they are especially susceptible to incorrect mapping due to minor alleles in the reference. In this example, we used the Peripheral Blood Mononuclear Cell dataset generated by the 10X Chromium v3 protocol. The changes in the gene expression between the pan-human and reference genomes are shown in Figure 4C for the T cell cluster. While the gene expression changes are small for the majority of the genes, several genes (red circles) exhibit a significant change in expression when minor alleles in the reference are replaced with major alleles (Supplementary Table 2). The genes that show increased expression (23 genes, 12 protein-coding, 7 disease-associated) in the pan-human consensus represent an improvement in sensitivity. On the other hand, the genes whose expression is higher in the reference (51 genes, 31 protein-coding, 22 disease-associated) are false positives that are eliminated in the consensus genome.

This effect can also be observed in the differential gene expression between the different clusters. Figure 4D shows how the differential gene expression between T cells and Monocytes changes when the reference is replaced with the

consensus genome. Although, as before, only several genes are impacted, the biological interpretation for such genes will be significantly altered by the consensus genome. Given these observations, we can conjecture that other gene-expression-based analyses, such as eQTL and TWAS, can also be improved by replacing the reference genome with the pan-human consensus. Furthermore, we found that analyses that go beyond gene expression, such as alternative splicing and differential isoform expression, are also noticeably affected by the reference replacement with the consensus.

## Discussion

In any data analysis, often a first central question is how much variation to include. This might be accomplished by dimension reduction, quality control, feature selection, stratification, or other techniques. The human genome is no exception, and considering how best it should be summarized remains a crucial problem. Crucially, that problem may have a use-dependent solution: what is essential for disease variant detection may not be necessary for RNA-seq alignment, and vice versa. The current reference genome has had enormous utility, and before tearing down the infrastructure that has been built up to exploit it, it is important to consider alternatives carefully. Graph genome methods are one promising option, and they resolve the primary deficiency in the reference: effectively incorporating all variation (or aspiring to). However, this comprehensiveness comes with its own host of issues, such as the lack of a simple coordinate system, difficulties with visualization, and significantly inflated computing requirements. The wide adoption of a graph-based reference genome will likely take a long time, given the history of switching from one version of the linear reference to the next: GRCh38 was released in December 2013 (<https://genome.ucsc.edu/FAQ/FAQreleases.html>), and at the time of this writing, seven years later, studies are still being published using GRCh37.

Although the full adoption of a graph genome may be several years in the future, the path there need not be a straight line. We may explore methods that partially improve on the current reference while imposing a fraction of the costs of the graph methods. By progressively assessing the role of population variation (in essence, moving from low principal

components to higher ones), we can develop intermediate forms moving from the current reference to more accurate reflections of population variation, particularly ones that still opt to summarize variability to some degree. The consensus genomes have substantial utility at the pan-human level and then show a fall off past that point, suggesting that the pan-human consensus can be considered a first step in the direction of adding population variation information to the reference. Although consensus genomes are unable to represent all human genotypic variation comprehensively, they are still a desirable alternative to the reference as they eliminate the millions of spurious minor alleles present in the current reference genome while maintaining a simple linear coordinate system.

Second-order approximations to the consensus reference have also been proposed. For instance, in the MajorFlow (Chen et al. 2021) algorithm, reads are mapped to a collection of reference genomes incorporating population variation, and the reference with the best alignment for each read is selected. Applying this methodology to RNA-seq data is an exciting possibility to be explored in future work.

Consensus genomes have a straightforward representation in graph genomes: the consensus sequence is the locally most probable linear path in the variation graph genome (i.e., the path where alternative variants with the highest population frequency are selected). Thus, consensus genomes can be thought of as a first-order approximation of the full variation graph genome. Graph-based aligners, such as VG (Hickey et al. 2020), HISAT2 (Kim et al. 2019), and minigraph (Li et al. 2020), have been shown to increase the accuracy of mapping. We can envision that after computing alignments as paths through the variation graph, these aligners can project the graph alignments into the linear consensus path, hence allowing for a more straightforward output, more compatible with the downstream processing pipelines.

This study explored the advantages and limitations of using consensus genomes for RNA-seq mapping. We used read alignments to the haploid personal genome as a proxy for the ground truth to quantify the rate of erroneous alignments to the reference genome and compared it to the three levels of consensus: pan-human, super-population, and population.

The overall mapping error rate caused by reference shortcomings is relatively small at only ~0.5-0.6% of all reads for the reference genome and further reduced to 0.3-0.4% for the consensus genomes, leaving relatively small room for further improvements (Figure 2D). However, for some analyses, such as allele-specific expression or de novo variant calling, the only reads of interest are those that overlap the variants. If we normalize the number of the erroneous reads by the number of reads that overlap the personal variants for each individual, we observe much higher corresponding error rates of ~8-10%, which decrease to ~2-4% when using a consensus genome.

The homozygous error rate (defined for reads that overlap only homozygous variants) is substantially decreased (by ~2-3 fold) when the pan-human consensus replaces the reference genome. Using the super-population or population consensus does not further improve the mapping accuracy, indicating that the pan-human consensus captures most population variation information that can be captured in a linear haploid genome. Using the super-population or population consensus genomes may not be worth the loss of generality: for instance, it will severely complicate interpopulation comparisons owing to the lack of a standard coordinate system.

These mapping results call into question the time and resources spent on constructing consensus genomes for particular populations (Cho et al. 2016; Fakhro et al. 2016; Higasa et al. 2016; Sherman et al. 2019; Takayama et al. 2021). Intuitively, one would expect that more specific consensus genomes would increase the mapping accuracy for the populations they represent. However, our results indicate that a universal pan-human consensus genome is sufficient to attain the best possible accuracy that can be achieved with a haploid reference, and the expensive efforts to construct more population-specific references are likely futile for improving the accuracy of RNA-seq analyses.

On the other hand, the heterozygous error rate (for reads that overlap heterozygous variants) is not significantly reduced by replacing the reference with a consensus of any population level. This is not surprising given that the haploid genome can only include one of the alleles of a heterozygous locus and hence cannot truthfully represent it. Graph genomes or other non-linear reference representations will be required to reduce error rates for heterozygous loci.

Although there is still work to be done on improving the reference genome, the pan-human consensus already offers noticeable improvements in downstream analyses, as indicated by the difference in splice junction expression quantification. We demonstrated that the accuracy of the splice junction quantification is significantly improved by switching from the reference to the pan-human consensus. These improvements imply important consequences in functional analyses such as alternative splicing, transcript abundance quantification, and differential isoform usage. Splice junction differences are subtle, but the 5-fold difference in the number of splice junctions with higher quantification error in the reference than in the pan-human consensus demonstrates that the pan-human consensus offers meaningful improvements over the reference. Results from a similar analysis of gene isoform expression (Supplementary Information) provide additional support for this claim.

At the same time, mapping to the consensus genome instead of the reference leads to marginal increases in computational time (~2%, Supplementary Figure S33) and memory (~10%, from 29GiB to 32GiB). These increases are driven mainly by the need to convert the consensus alignment coordinates to the reference coordinates, which will be eliminated if the consensus genome becomes the reference.

This study was focused on the benefits of a consensus reference for RNA-seq analyses. To illustrate that these results can be generalized for other types of functional sequencing assays, we calculated mapping error rates for the H3K4me3 histone modification ChIP-seq dataset from the ENCODE consortium (Supplementary Figure S37). Similar to the RNA-seq results, the error rate for reads overlapping homozygous variants is reduced from 6.1% to 1.9% when the reference is replaced with the pan-human consensus, while population-specific consensus do not improve the accuracy significantly.

This study only considered single nucleotide variants and small insertions/deletions in this study. Large structural variants can add or remove large sequence fragments from the genome (Sherman et al. 2019) and thus may have an even bigger effect on mapping accuracy. The new generation of long-read technologies shows promise for the confident detection of



large structural variants. However, at this time, allele frequency information is unavailable for large structural variants, and thus they cannot be included in the consensus reference construction.

Ultimately, the best reference sequence for each individual is their own personal genome. As sequencing costs are rapidly decreasing, personal genomes are becoming more available. Nevertheless, there will be a need for a common reference capable of representing the analysis results in the universal coordinate system.

The pan-human consensus appears to be a strict improvement over the current reference with minimal costs, and thus we propose replacing the current reference with the pan-human consensus. Besides the question of absolute utility, we also advocate using consensus genomes as a mechanism to develop practices to improve genome representation more generally. Recent years have seen genomics pipelines using the reference become entrenched, to varying degrees, by researchers unwilling to upgrade. Because the consensus genome requires minor changes in pipelines, it can be used as a straightforward, first-order approximation to assess and explore the sensitivity of specific genomic analyses to genome variation. For instance, the benefits of the consensus genome for RNA-seq mapping can be explored via the STAR-consensus pipeline, which aligns reads to the consensus genome and then transforms the coordinates to the reference genome coordinates, thus eliminating the need for changes in the downstream processing. By incorporating consensus genomes, we envision not only improvements in the absolute performance of diverse research projects but also a greater understanding of the dependencies in those methods, thus setting the stage for a more flexible and robust future for genomics.

## Methods

### Calculating consensus alleles

We calculated the consensus allele for each variant on a per-haplotype basis: the number of occurrences of each allele was counted, and the most common allele was selected. For the pan-human consensus, the alleles were counted across all individuals. For each super-population and population consensus, the alleles were counted across all individuals within that group. This counting was performed in Python by ConsDB, by reading through each VCF file one line at a time and parsing the genotype for each individual in the group for which the consensus is being constructed.

### Genome generation and read mapping

All genomes generation and read mapping were done with STAR v2.7.7a (Dobin et al. 2013). We used GRCh38 (Schneider et al. 2017) as the reference FASTA file and GENCODE v29 (Frankish et al. 2019) as the reference GTF file. We masked the PAR regions on the Y Chromosome to avoid any sex-based differences in mapping. For the generation of consensus and personal haploid genomes, we used the `--genomeTransformType Haploid` option and the `--genomeTransformVCF` option with the appropriate VCF file. For the read mapping, we used the `--genomeTransformOutput SAM SJ` and the `--quantMode GeneCounts TranscriptomeSAM` options. We also used the `--outSAMreadID Number` option in order to keep track of reads in the analysis steps more easily. Other than these options, we used the default STAR parameters.

### Mapping error calculations

Before calculating the mapping error, we made several preparations. First, we used `awk` to construct VCF files that contained only the individual's phased genotype. Next, we used these full VCFs to partition the variants for each consensus genome for each individual into four separate VCF files: one for homozygous SNPs, one for heterozygous SNPs, one for homozygous indels, and one for heterozygous indels. These four split VCFs needed to be generated for each

individual, including individuals from within the same population, because variants may be homozygous in one individual but heterozygous in a different individual.

For each individual, filtered alignments for the reference, pan-human consensus, super-population consensus, and population consensus were compared to the filtered alignment for their personal haploid genome using an awk script. We compared the genomes on a per-read basis, checking for differences in mapping position and number of mapped loci. To determine what types of variants each read overlapped, we overlapped the filtered BAM files with each of the four split VCF files using BEDTools, for each genome and each individual. We compared the read IDs from this overlap with the read IDs obtained from the genome mapping comparisons using grep in order to find error-causing variants.

The final steps of read counting and plotting were done using a Python script. For each individual, we summed the read counts for each combination of error type and homozygous/heterozygous variants across all four genomes being analyzed. The two normalization constants used for these figures were the total number of mapped reads for each individual and the total number of reads that overlapped personal homozygous variants. The total mapped read numbers were extracted from the STAR Log.final.out file. The counts of reads overlapping personal homozygous variants were found by counting the number of reads present in the previously found overlap files for reads overlapping homozygous variants in the personal haploid genome.

We applied the same mapping error calculation methodology to the ENCODE H3K4me3 ChIP-seq dataset for the GM12878 cell line derived from the 1000 Genomes individual NA12878. The FASTQ files ENCF598WCX, ENCF825QGB were downloaded from the ENCODE portal. STAR was run with an additional `-alignIntronMax 1` option to prohibit spliced alignments.

### Special considerations for reads aligned with HISAT2

Because HISAT2 does not have the same consensus-to-reference transformation capabilities as STAR-Consensus, the mapping error calculation pipeline must be adjusted to work with HISAT2. First, each individual's personal VCF file and all consensus VCF files were collapsed to remove overlapping variants, following the same procedure that the BCFtools

consensus command uses. This variant filtering was done using a custom Python script available in the accompanying GitHub repository. Following the VCF filtering, a FASTA file was generated for each individual and each consensus using these reduced VCF files with BCFtools. At this point, the standard HISAT2 index-generation and mapping commands were utilized. Since the coordinate system for the HISAT2 alignments was specific for each genome used, we used levioSAM (Mun et al. 2021) in conjunction with the previously generated VCF files to transform the alignment coordinates back to the reference. Other than this liftOver step, the comparison of alignments was identical to the pipeline used with the STAR-Consensus results.

### Simulating reads with personal variants

We used the following procedure to simulate personal reads and compare their alignments to the consensus genomes with the true coordinates. First, the sequences of all annotated transcripts were extracted from the reference genome, and each base of these sequences was associated with the reference coordinate. Next, we modified the transcript sequences for each individual using their personal single-nucleotide variants and indels, both homo- and heterozygous, which resulted in two haplotypes for each transcript. We then extracted the 50b read sequences from both personal haplotypes, covering all transcripts uniformly. The true coordinates of these reads in the reference genome were taken from the information recorded in the first step. Sequences that appeared multiple times in the personal genome were eliminated. Finally, we aligned the reads to the consensus genomes using STAR-Consensus, and transformed the alignments to the reference coordinates, allowing us to compare their mapped positions to the true simulated coordinates.

### Finding error-causing variant locations

To find the genomic annotations of error-causing variants, we first selected the error-causing variants as described above. We next used BEDTools to intersect these variants with the GENCODE v29 (Frankish et al. 2019) GTF file and find all genomic annotations that each variant overlaps. Because certain genomic annotations always fall within other genomic annotations (e.g., an exon will necessarily be located within a gene), a given variant is likely to have multiple

genomic annotations that it overlaps. We used a Python script to determine the most specific genomic annotation overlapped by each variant and count the number of variants falling within each type of genomic annotation.

### Processing single-cell RNA-seq dataset

We used the STARsolo gene/count matrix generated with `--soloFeatures GeneFull_ExonOverIntron` option as a starting point for the SCANPY (Wolf et al. 2018) 1.6.0 pipeline. We used the Leiden clustering algorithm to identify four main clusters: T cells, B cells, Natural killer (NK) cells, and Monocytes. The differentially expressed genes in each cluster were evaluated using SCANPY's implementation of the *t*-test.

### Software Availability

The ConsDB package is available on GitHub at <https://github.com/kaminow/consdb>. STAR-consensus is available at <https://github.com/alexdobin/star>. Scripts to reproduce the analysis in this study, including the Supplementary Information/Figures, are available at [https://github.com/kaminow/ConsDB\\_analysis](https://github.com/kaminow/ConsDB_analysis).

## Competing interest statement

The authors declare no competing interests.

## Acknowledgments

Research reported in this publication/press was supported by the National Human Genome Research Institute, National Institute Of Mental Health, and National Library Of Medicine of the National Institutes of Health under awards R01HG009318 (B.K. and A.D.), R01MH113005 (S.B. and J.G.) and R01LM012736 (S.B. and J.G.). The content is solely the responsibility of the authors and does not necessarily represent the official views of the National Institutes of Health. S.B. was also supported by a generous donation from the Magid family.

## Author Contributions

Benjamin Kaminow: Conceptualization, Methodology, Software, Formal analysis, Investigation, Data Curation, Writing – original draft preparation, Writing – review and editing, Visualization

Sara Ballouz: Conceptualization, Methodology, Writing – review and editing

Jesse Gillis: Conceptualization, Methodology, Writing – review and editing

Alexander Dobin: Conceptualization, Methodology, Software, Writing – review and editing, Supervision

## References

- Assembly Releases and Versions*. 2020. UCSC Genome Browser. <https://genome.ucsc.edu/FAQ/FAQreleases.html>
- Balasubramanian S, Habegger L, Frankish A, MacArthur DG, Harte R, Tyler-Smith C, Harrow J, Gerstein M. 2011. Gene inactivation and its implications for annotation in the era of personal genomics. *Genes Dev* **25**: 1–10.
- Ballouz S, Dobin A, Gillis JA. 2019. Is it time to change the reference genome? *Genome Biol* **20**: 159. <https://doi.org/10.1186/s13059-019-1774-4>
- Barbitoff YA, Bezdvornykh IV, Polev DE, Serebryakova EA, Glotov AS, Glotov OS, Predeus AV. 2018. Catching hidden variation: Systematic correction of reference minor allele annotation in clinical variant calling. *Genet Med* **20**: 360–364.
- Berlin K, Koren S, Chin CS, Drake JP, Landolin JM, Phillippy AM. 2015. Assembling large genomes with single-molecule sequencing and locality-sensitive hashing. *Nat Biotechnol* **33**: 623–630.
- Buchkovich ML, Eklund K, Duan Q, Li Y, Mohlke KL, Furey TS. 2015. Removing reference mapping biases using limited or no genotype data identifies allelic differences in protein binding at disease-associated loci. *BMC Medical Genom*, **8**: 43. <https://doi.org/10.1186/s12920-015-0117-x>
- Castel SE, Levy-Moonshine A, Mohammadi P, Banks E, Lappalainen T. 2015. Tools and best practices for data processing in allelic expression analysis. *Genome Biol* **16**: 195. <https://doi.org/10.1186/s13059-015-0762-6>
- Chen N-C, Solomon B, Mun T, Iyer S, Langmead B. 2021. Reference flow: Reducing reference bias using multiple population genomes. *Genome Biol* **22**: <https://doi.org/10.1186/s13059-020-02229-3>
- Chen R, Butte AJ. 2011. The Reference Human Genome Demonstrates High Risk of Type 1 Diabetes and Other Disorders. *Pacific Symposium on Biocomputing*. *Pacific Symposium on Biocomputing*, 231–242.
- Cho YS, Kim H, Kim HM, Jho S, Jun J, Lee YJ, Chae KS, Kim CG, Kim S, Eriksson A, et al. 2016. An ethnically relevant consensus Korean reference genome is a step towards personal reference genomes. *Nat Commun* **7**: 13637. <https://doi.org/10.1038/ncomms13637>
- Church DM, Schneider VA, Steinberg KM, Schatz MC, Quinlan AR, Chin CS, Kitts PA, Aken B, Marth GT, Hoffman MM, et al. 2015. Extending reference assembly models. *Genome Biol* **16**: 13. <https://doi.org/10.1186/s13059-015-0587-3>
- Clarke L, Fairley S, Zheng-Bradley X, Streeter I, Perry E, Lowy E, Tassé AM, Flicek P. 2017. The international Genome sample resource (IGSR): A worldwide collection of genome variation incorporating the 1000 Genomes Project data. *Nucleic Acids Res* **45**: D854–D859.
- Danecek P, Bonfield JK, Liddle J, Marshall J, Ohan V, Pollard MO, Whitwham A, Keane T, McCarthy SA, Davies RM, Li H. 2021. Twelve years of SAMtools and BCFtools. *GigaScience* **10**. <https://doi.org/10.1093/gigascience/giab008>
- Dewey FE, Chen R, Cordero SP, Ormond KE, Caleshu C, Karczewski KJ, Whirl-Carrillo M, Wheeler MT, Dudley JT, Byrnes JK, et al. 2011. Phased Whole-Genome Genetic Risk in a Family Quartet Using a Major Allele Reference Sequence. *PLoS Genet* **7**: 9. <https://doi.org/10.1371/journal.pgen.1002280>
- Dobin A, Davis CA, Schlesinger F, Drenkow J, Zaleski C, Jha S, Batut P, Chaisson M, Gingeras TR. 2013. STAR: Ultrafast universal RNA-seq aligner. *Bioinformatics* **29**: 15–21.
- Fairley S, Lowy-Gallego E, Perry E, Flicek P. 2020. The International Genome Sample Resource (IGSR) collection of open human genomic variation resources. *Nucleic Acids Res* **48**: D941–D947.
- Fakhro KA, Staudt MR, Ramstetter MD, Robay A, Malek JA, Badii R, Al-Marri AAN, Khalil CA, Al-Shakaki A, Chidiac O, et al. 2016. The Qatar genome: A population-specific tool for precision medicine in the Middle East. *Hum Genome Var* **3**: 1–7.
- Frankish A, Diekhans M, Ferreira AM, Johnson R, Jungreis I, Loveland J, Mudge JM, Sisu C, Wright J, Armstrong J, et al. 2019. GENCODE reference annotation for the human and mouse genomes. *Nucleic Acids Res*, **47**: D766–D773.
- Frequently Asked Questions*. 2020. Genome Reference Consortium. <https://www.ncbi.nlm.nih.gov/grc/help/faq/>

- Garrison E, Sirén J, Novak AM, Hickey G, Eizenga JM, Dawson ET, Jones W, Garg S, Markello C, Lin MF, et al. 2018. Variation graph toolkit improves read mapping by representing genetic variation in the reference. *Nat Biotechnol* **36**: 875–879.
- Hickey G, Heller D, Monlong J, Sibbesen JA, Sirén J, Eizenga J, Dawson ET, Garrison E, Novak AM, Paten B. 2020. Genotyping structural variants in pangenome graphs using the VG toolkit. *Genome Biol* **21**: <https://doi.org/10.1186/s13059-020-1941-7>
- Higasa K, Miyake N, Yoshimura J, Okamura K, Niihori T, Saitsu H, Doi K, Shimizu M, Nakabayashi K, Aoki Y, et al. 2016. Human genetic variation database, a reference database of genetic variations in the Japanese population. *J Hum Genet* **61**: 547–553.
- Human Genome Overview*. 2020. Genome Reference Consortium. <https://www.ncbi.nlm.nih.gov/grc/human>
- Human Genome Project FAQ*. 2020. National Human Genome Research Institute. <https://www.genome.gov/human-genome-project/Completion-FAQ>
- International Human Genome Sequencing Consortium. 2004. Finishing the euchromatic sequence of the human genome. *Nature* **431**: 931–945.
- Ionita-Laza I, Lange C, Laird NM. 2009. Estimating the number of unseen variants in the human genome. *PNAS* **106**: 5008–5013.
- Karczewski KJ, Francioli LC, Tiao G, Cummings BB, Alföldi J, Wang Q, Collins RL, Laricchia KM, Ganna A, Birnbaum DP, et al. 2020. The mutational constraint spectrum quantified from variation in 141,456 humans. *Nature* **581**: 434–443.
- Karthikeyan S, Bawa PS, Srinivasan S. 2016. hg19K: Addressing a significant lacuna in hg19-based variant calling. *Mol Genet Genom Med* **5**: 15–20.
- Kim D, Paggi JM, Park C, Bennett C, Salzberg SL. 2019. Graph-based genome alignment and genotyping with HISAT2 and HISAT-genotype. *Nat Biotechnol* **37**: 907–915. <https://doi.org/10.1038/s41587-019-0201-4>
- International Human Genome Sequencing Consortium. 2001. Initial sequencing and analysis of the human genome. *Nature* **409**: 860–921.
- Lappalainen T, Sammeth M, Friedländer MR, 't Hoen PA, Monlong J, Rivas MA, González-Porta M, Kurbatova N, Griebel T, Ferreira PG, et al. 2013. Transcriptome and genome sequencing uncovers functional variation in humans. *Nature* **501**: 506–511. <https://doi.org/10.1038/nature12531>
- Li B, Dewey CN. 2011. RSEM: Accurate transcript quantification from RNA-Seq data with or without a reference genome. *BMC Bioinformatics* **12**: 323. <https://doi.org/10.1186/1471-2105-12-323>
- Li H, Feng X, Chu C. 2020. The design and construction of reference pangenome graphs with minigraph. *Genome Biol*, **21**. <https://doi.org/10.1186/s13059-020-02168-z>
- Mahmoud M, Gobet N, Cruz-Dávalos DI, Mounier N, Dessimoz C, Sedlazeck FJ. 2019. Structural variant calling: The long and the short of it. *Genome Biol* **20**: 246. <https://doi.org/10.1186/s13059-019-1828-7>
- Mun T, Chen N-C, Langmead B. 2021. LevioSAM: Fast lift-over of variant-aware reference alignments. *Bioinformatics* **37**: 4243–4245. <https://doi.org/10.1093/bioinformatics/btab396>
- Overview of Structural Variation*. 2020. National Center for Biotechnology Information. <https://www.ncbi.nlm.nih.gov/dbvar/content/overview>
- Paten B, Novak AM, Eizenga JM, Garrison E. 2017. Genome graphs and the evolution of genome inference. *Genome Res* **27**: 665–676.
- Piñero J, Bravo À, Queralt-Rosinach N, Gutiérrez-Sacristán A, Deu-Pons J, Centeno E, García-García J, Sanz F, Furlong LI. 2016. DisGeNET: A comprehensive platform integrating information on human disease-associated genes and variants. *Nucleic Acids Res* **45**: <https://doi.org/10.1093/nar/gkw943>
- Pritt J, Chen NC, Langmead B. 2018. FORGe: Prioritizing variants for graph genomes. *Genome Biol* **19**: 220. <https://doi.org/10.1186/s13059-018-1595-x>
- Rakocevic G, Semenyuk V, Lee WP, Spencer J, Browning J, Johnson IJ, Arsenijevic V, Nadj J, Ghose K, Suci MC, et al. 2019. Fast and accurate genomic analyses using genome graphs. *Nat Genet* **51**: 354–362.
- Rosenfeld JA, Mason CE, Smith TM. 2012. Limitations of the Human Reference Genome for Personalized Genomics. *PLoS ONE* **7**: 7. <https://doi.org/10.1371/journal.pone.0040294>



- Schneider VA, Graves-Lindsay T, Howe K, Bouk N, Chen H-C, Kitts PA, Murphy TD, Pruitt KD, Thibaud-Nissen F, Albracht D, et al. 2017. Evaluation of GRCH38 and de novo haploid genome assemblies demonstrates the enduring quality of the Reference Assembly. *Genome Res* **27**: 849–864. <https://doi.org/10.1101/gr.213611.116>
- Sherman RM, Forman J, Antonescu V, Puiu D, Daya M, Rafaels N, Boorgula MP, Chavan S, Vergara C, Ortega VE, et al. 2019. Assembly of a pan-genome from deep sequencing of 910 humans of African descent. *Nat Genet* **51**: 30–35.
- Sherry ST, Ward MH, Kholodov M, Baker J, Phan L, Smigielski EM, Sirotkin K. 2001. dbSNP: The NCBI database of genetic variation. *Nucleic Acids Res* **29**: 308–311.
- Shukla HG, Bawa PS, Srinivasan S. 2019. hg19KIndel: Ethnicity normalized human reference genome. *BMC Genomics* **20**: 459. <https://doi.org/10.1186/s12864-019-5854-3>
- Sirén J, Monlong J, Chang X, Novak AM, Eizenga JM, Markello C, Sibbesen JA, Hickey G, Chang P-C, Carroll A, et al. 2021. Pangenomics enables genotyping of known structural variants in 5202 diverse genomes. *Science*, **374**. <https://doi.org/10.1126/science.abg8871>
- Stevenson KR, Coolon JD, Wittkopp PJ. 2013. Sources of bias in measures of allele-specific expression derived from RNA-seq data aligned to a single reference genome. *BMC Genomics* **14**: 536. <https://doi.org/10.1186/1471-2164-14-536>
- Takayama J, Tadaka S, Yano K, Katsuoka F, Gocho C, Funayama T, Makino S, Okamura Y, Kikuchi A, Sugimoto S, et al. 2021. Construction and integration of three de novo Japanese human genome assemblies toward a population-specific reference. *Nat Commun* **12**. <https://doi.org/10.1038/s41467-020-20146-8>
- The 1000 Genomes Project Consortium. 2015. A global reference for human genetic variation. *Nature* **526**: 68–74.
- Valenzuela D, Norri T, Välimäki N, Pitkänen E, Mäkinen V. 2018. Towards pan-genome read alignment to improve variation calling. *BMC Genomics* **19**: 87. <https://doi.org/10.1186/s12864-018-4465-8>.
- Wolf FA, Angerer P, Theis FJ. 2018. SCANPY: Large-scale single-cell gene expression data analysis. *Genome Biol* **19**. <https://doi.org/10.1186/s13059-017-1382-0>

## Figures

### Figure 1:

**A)** Construction of a consensus genome: the minor allele in the reference is replaced by the most common (major) allele in the population.

**B)** Visual representation of the individuals used to construct consensus genomes of varying population specificity.

**C)** ConsDB workflow.

**D)** Number of major alleles for each population consensus genome that were replaced in the reference.

**E)** Number of SNPs and indels shared between different combinations of the pan-human, super-population, and population consensus genomes for the African population. The bars in the top bar plot show the number of SNPs and indels that are unique to the intersection of genomes indicated in the dot matrix below. The horizontal bars on the bottom left show the total number of SNPs and indels present in each genome.

**F)** Number of SNPs and indels shared between different combinations of the pan-human consensus and all three super-population consensus genomes. The bars in the top bar plot show the number of SNPs and indels that are unique to the intersection of genomes indicated in the dot matrix below. The horizontal bars on the bottom left show the total number of SNPs and indels present in each genome.

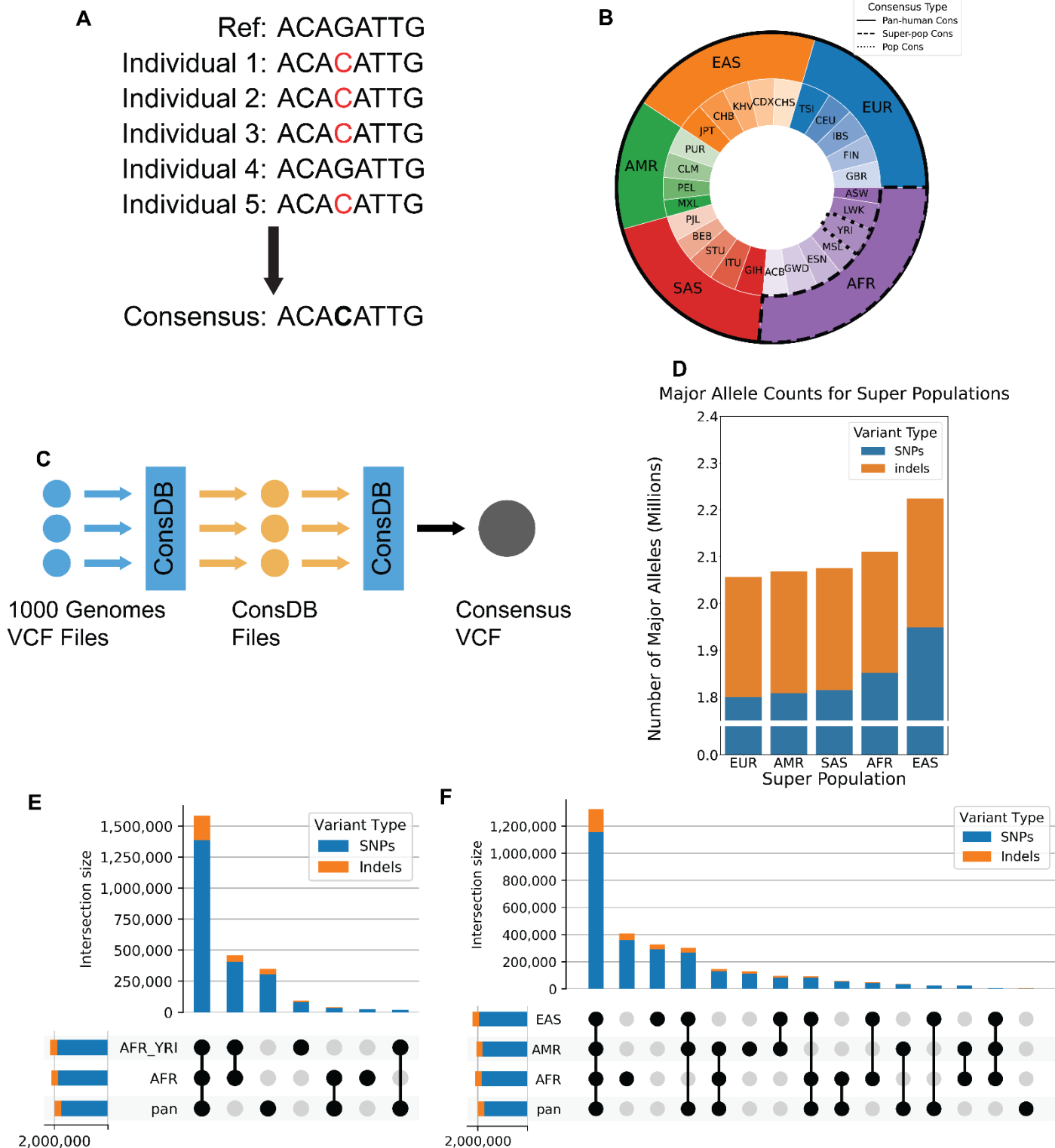


**Figure 2:** Mapping accuracy improvements due to switching from reference to consensus genomes.

**A)** Internal workflow of STAR-consensus.

**B)** Different types of mapping errors based on the read's mapping status in the individual's haploid personal genome and the reference or given consensus genome.

**C)** Overall mapping error rate for each error type for individual NA19238. Genome is shown on the x-axis and the mapping error rate is shown on the y-axis.

**D)** Overall mapping error rate for all individuals. Individuals from the same population are grouped together by color, with each marker shape representing one individual in the population. The dashed line shows the average error rate for the population, and the solid vertical line indicates the range of the population.

**E)** Homozygous mapping error rate for each error type for individual NA19238.

**F)** Homozygous mapping error rate for all individuals. Individuals from the same population are grouped together by color, with each marker shape representing one individual in the population. The dashed line shows the average error rate for the population, and the solid vertical line indicates the range of the population.

**G)** Homozygous mapping error rates for each error type for simulated reads for individual NA12938.

**H)** Population-average homozygous mapping error rates for simulated reads for all individuals.

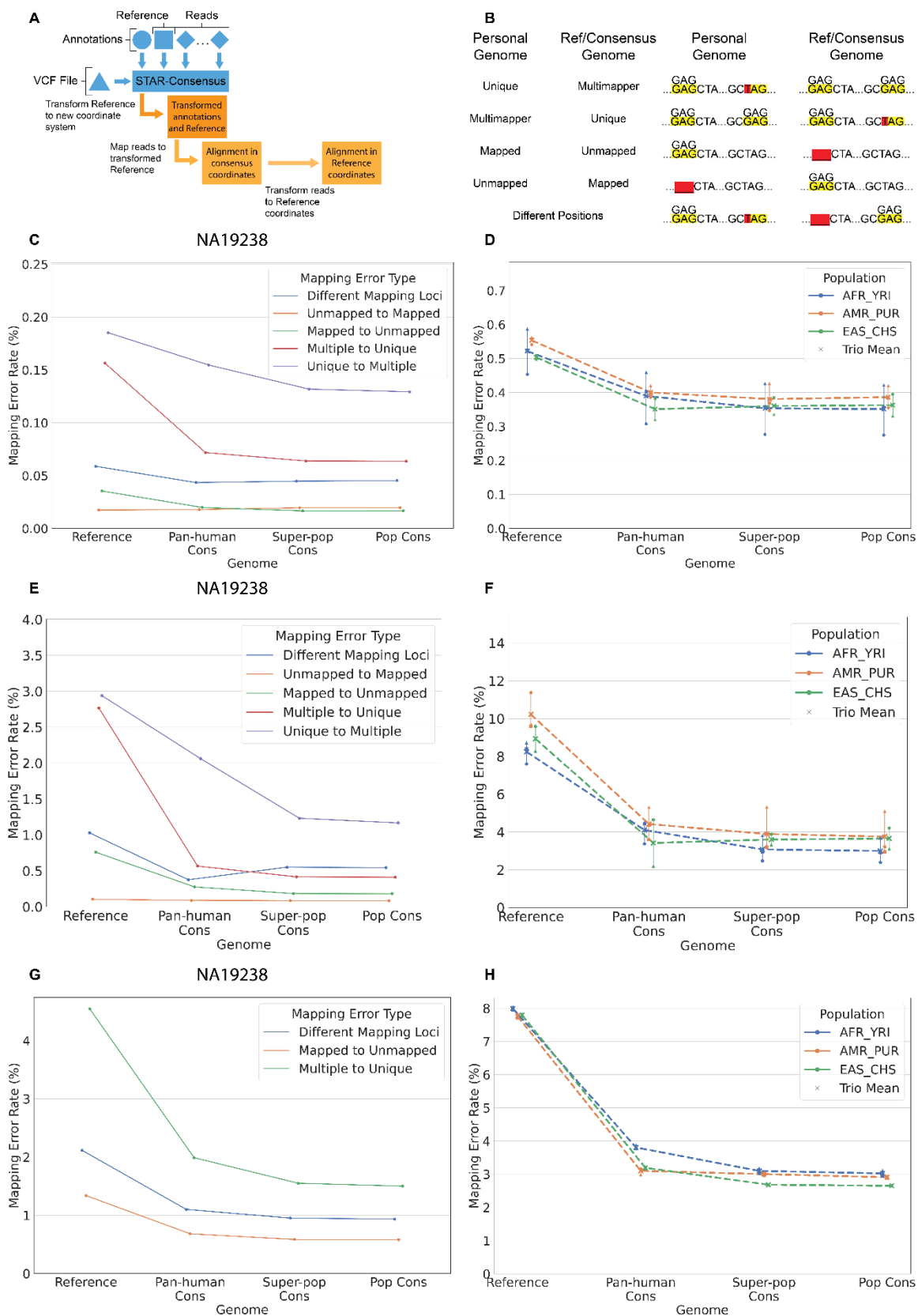


**Figure 3:** Mapping accuracy improvements due to switching from reference to consensus genomes when mapping to alternative genomes.

**A)** Each individual from each population is independently mapped to the reference, pan-human consensus, and all population and super-population consensus genomes.

**B)** Homozygous mapping error rate when mapping to different consensus. The color of the marker indicates the population to which that individual belongs, while the shape of the marker identifies the individual within the trio. The color of the background rectangle indicates the population of the genome. The dashed line in each column represents the mean mapping error for that combination of genome and individuals.

**C)** Each individual from each population is independently mapped to the reference, pan-human consensus, and all personal haploid genomes.

**D)** Homozygous mapping error rate when mapping to different personal haploid genomes.

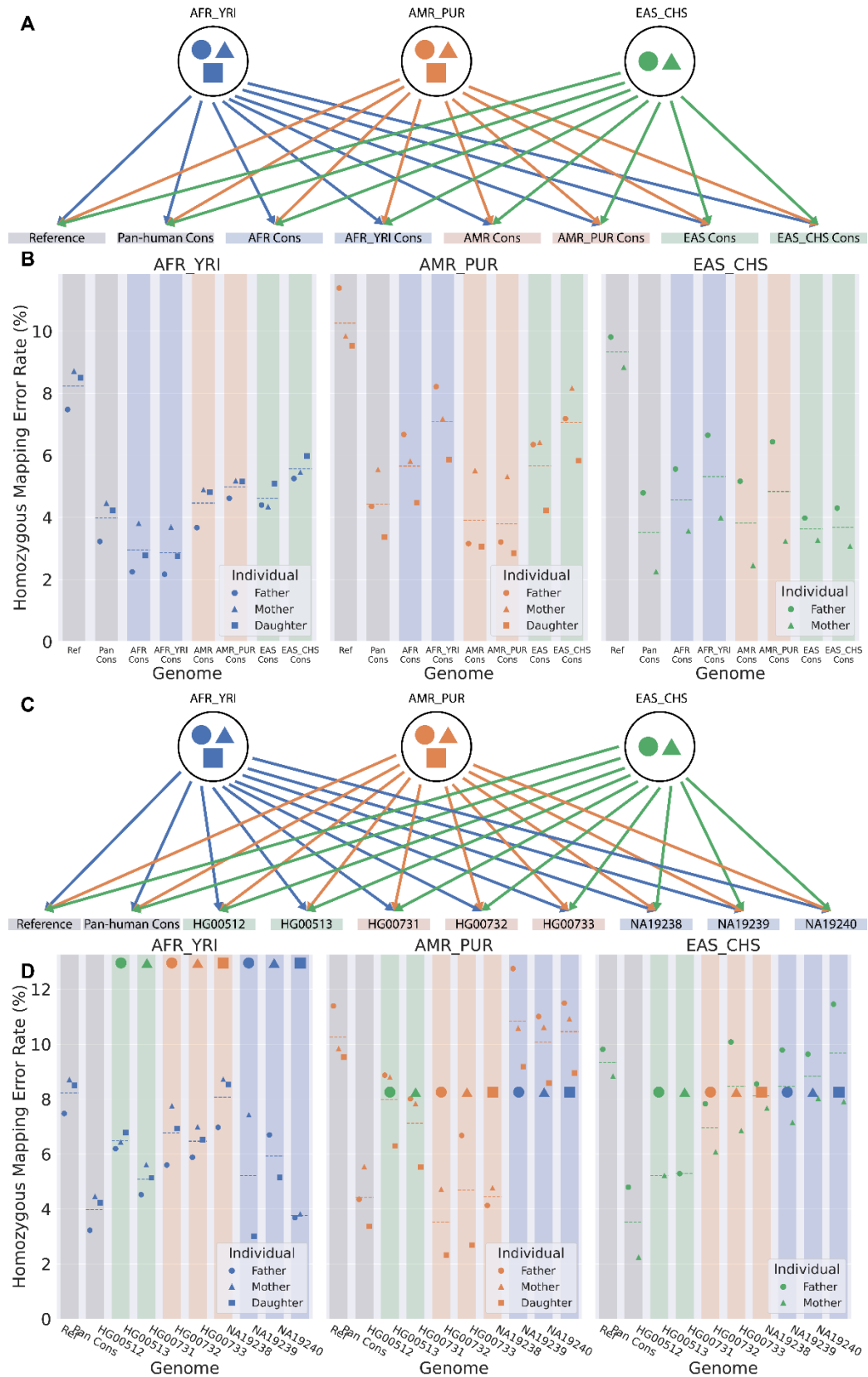


**Figure 4:** Functional effects of replacing the reference genome with a consensus.

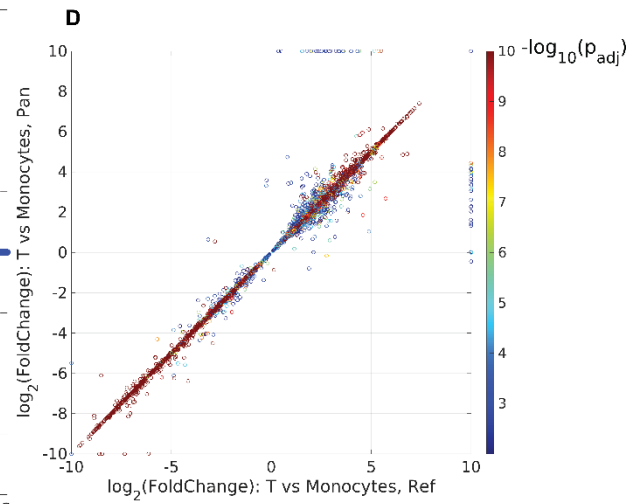
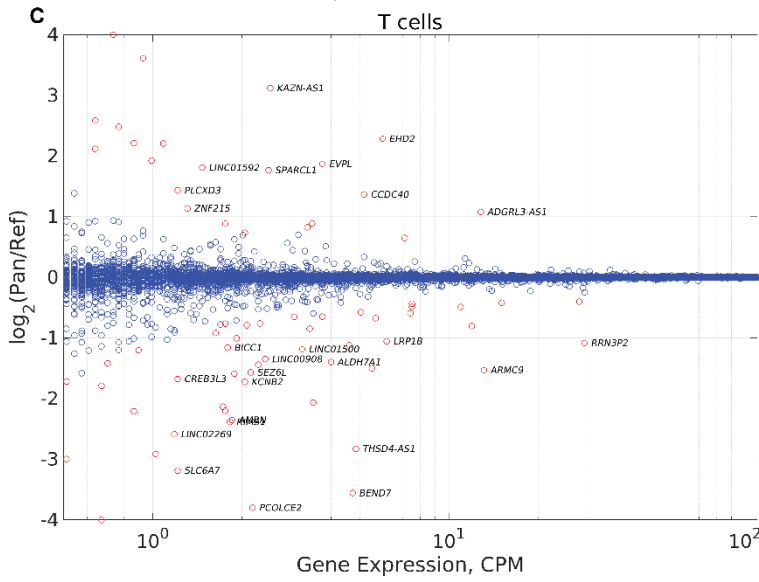
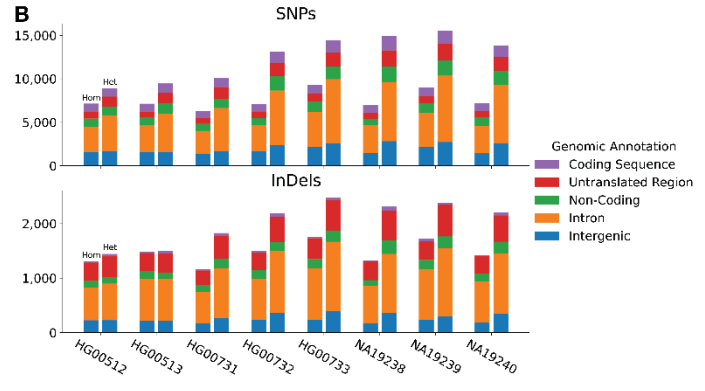
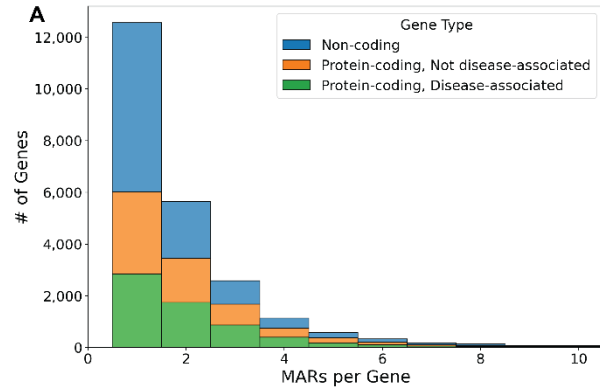
**A)** Histogram of the number of MARs in the exons of non-coding, protein-coding, and disease-associated genes.

**B)** Counts of variants in the personal haploid genome that cause mapping errors in the reference, classified by the genomic feature in which the variant is located. For each set of bars, the left bar shows the number of homozygous variants and the right bar indicates the number of heterozygous variants.

**C)** The gene expression log<sub>2</sub> fold change between the pan-human consensus and the reference genome as a function of the maximum expression in counts per million of the T cell cluster. Red circles indicate genes with an adjusted p-value < 0.1.

**D)** Comparison of the gene expression log<sub>2</sub> fold change between T cells and Monocytes in the pan-human consensus and the reference genome. The log<sub>2</sub> fold change values were capped between -10 and 10.







## Pan-human consensus genome significantly improves the accuracy of RNA-seq analyses

Benjamin Kaminow, Sara Ballouz, Jesse Gillis, et al.

*Genome Res.* published online March 7, 2022

Access the most recent version at doi:[10.1101/gr.275613.121](https://doi.org/10.1101/gr.275613.121)

---

<b>P&lt;P</b>	Published online March 7, 2022 in advance of the print journal.
<b>Accepted Manuscript</b>	Peer-reviewed and accepted for publication but not copyedited or typeset; accepted manuscript is likely to differ from the final, published version.
<b>Open Access</b>	Freely available online through the <i>Genome Research</i> Open Access option.
<b>Creative Commons License</b>	This manuscript is Open Access. This article, published in <i>Genome Research</i> , is available under a Creative Commons License (Attribution 4.0 International license), as described at <a href="http://creativecommons.org/licenses/by/4.0/">http://creativecommons.org/licenses/by/4.0/</a> .
<b>Email Alerting Service</b>	Receive free email alerts when new articles cite this article - sign up in the box at the top right corner of the article or <a href="#">click here</a> .

---

Affordable, Accurate  
Sequencing.



---

To subscribe to *Genome Research* go to:  
<https://genome.cshlp.org/subscriptions>

---